

## POWER ASYMMETRY IN *WMAP* AND *PLANCK* TEMPERATURE SKY MAPS AS MEASURED BY A LOCAL VARIANCE ESTIMATOR

Y. AKRAMI<sup>1</sup>, Y. FANTAYE<sup>1,2</sup>, A. SHAFIELOO<sup>3,4</sup>, H. K. ERIKSEN<sup>1</sup>, F. K. HANSEN<sup>1</sup>, A. J. BANDAY<sup>5,6</sup>, AND K. M. GÓRSKI<sup>7,8</sup>

*Draft version March 25, 2014*

### ABSTRACT

We revisit the question of hemispherical power asymmetry in the *WMAP* and *Planck* temperature sky maps by measuring the local variance over the sky and on disks of various sizes. For the 2013 *Planck* sky map we find that none of the 1000 available isotropic *Planck* “Full Focal Plane” simulations have a larger variance asymmetry than that estimated from the data, suggesting the presence of an anisotropic signature formally significant at least at the  $3.3\sigma$  level. For the *WMAP* 9-year data we find that 5 out of 1000 simulations have a larger asymmetry. The preferred direction for the asymmetry from the *Planck* data is  $(l, b) = (212^\circ, -13^\circ)$ , in good agreement with previous reports of the same hemispherical power asymmetry.

*Subject headings:* cosmic microwave background — cosmology: observations — methods: statistical

### 1. INTRODUCTION

The assumptions of statistical isotropy and homogeneity of the Universe on very large scales, jointly called the cosmological principles, are two of the main pillars of our present standard model of cosmology. In the past, the validity of these assumptions was based largely on philosophical arguments, or as a necessity in order to simplify otherwise complicated equations. Today, the situation is very different. With the advent of advanced space and ground-based instruments, stringent tests of these basic assumptions are available.

Indeed, almost immediately after the first release of the measurements of the cosmic microwave background (CMB) temperature fluctuations by the *Wilkinson Microwave Anisotropy Probe* (*WMAP*) experiment (Bennett et al. 2003), different groups found various anomalous features in the data that hinted at possible violations of the statistical isotropy (see, e.g., Tegmark et al. 2003; de Oliveira-Costa et al. 2004; Vielva et al. 2004; Larson & Wandelt 2004; Land & Magueijo 2005a,b; McEwen et al. 2005, 2006; Jaffe et al. 2006; Hinshaw et al. 2007; Spergel et al. 2007; Cruz et al. 2007; Bridges et al. 2007; Copi et al. 2007; Land & Magueijo 2007; Bernui et al. 2007; Bernui & Hipolito-Ricaldi 2008; Pietrobon et al. 2008). Among these was one suggesting a directional de-

pendency of the CMB angular power spectrum (Eriksen et al. 2004; Hansen et al. 2004), often referred to as a “hemispherical power asymmetry”. Since then, this observation has been probed with different methods and algorithms, and is with current data sets generally found to be statistically significant at the  $3\sigma - 3.5\sigma$  level depending on the algorithm and angular scales under considerations (Park 2004; Eriksen et al. 2007; Hansen et al. 2009; Hoftuft et al. 2009; Axelsson et al. 2013; Planck Collaboration 2013d). Accordingly, theorists are now attempting to reconcile these observations with the current cosmological standard model (see, e.g., Ericcek et al. 2008; Dai et al. 2013; Lyth 2013; Liu et al. 2013; Liddle & Corts 2013; Mazumdar & Wang 2013; Namjoo et al. 2013; Abolhasani et al. 2013; Cai et al. 2013; Kohri et al. 2013; McDonald 2013; Kanno et al. 2013).

Gordon et al. (2005) suggested that the power asymmetry might be modeled in terms of a dipole modulation of the form

$$\frac{\Delta T}{T}|_{\text{mod}}(\hat{n}) = (1 + A \hat{n} \cdot \hat{p}) \frac{\Delta T}{T}|_{\text{iso}}(\hat{n}), \quad (1)$$

where  $\frac{\Delta T}{T}|_{\text{iso}}$  and  $\frac{\Delta T}{T}|_{\text{mod}}$  are, respectively, the isotropic and modulated CMB temperature fluctuations along a direction  $\hat{n}$  on the sky,  $A$  is the amplitude of the dipole modulation and  $\hat{p}$  is the preferred direction. Direct likelihood fits of this particular model have been reported by Eriksen et al. (2007); Hoftuft et al. (2009); Planck Collaboration (2013d) for the *WMAP* and *Planck* (Planck Collaboration 2013a) data, obtaining a typical dipole modulation amplitude of  $A \sim 0.07$  on large angular scales, statistically significant at  $\sim 3\sigma$ . Equivalent results have been obtained using for instance the BiPolar Spherical Harmonics (BiPoSHs) technique (Hajian & Souradeep 2003, 2006; Planck Collaboration 2013d). On small angular scales, the dipole amplitude is much lower, and appears to vanish by a multipole moment of  $\ell \sim 500-600$  (Hansen et al. 2009; Planck Collaboration 2013d).

However, there is a significant debate in the field concerning whether these findings are statistically signifi-

yashar.akrami@astro.uio.no  
y.t.fantaye@astro.uio.no  
arman@apctp.org

<sup>1</sup> Institute of Theoretical Astrophysics, University of Oslo, P.O. Box 1029 Blindern, N-0315 Oslo, Norway

<sup>2</sup> Department of Mathematics, University of Rome Tor Vergata, Rome, Italy

<sup>3</sup> Asia Pacific Center for Theoretical Physics, Pohang, Gyeongbuk 790-784, Korea

<sup>4</sup> Department of Physics, POSTECH, Pohang, Gyeongbuk 790-784, Korea

<sup>5</sup> Université de Toulouse, UPS-OMP, IRAP, F-31028 Toulouse cedex 4, France

<sup>6</sup> CNRS, IRAP, 9 Av. Colonel Roche, BP 44346, F-31028 Toulouse cedex 4, France

<sup>7</sup> Jet Propulsion Laboratory, California Institute of Technology, 4800 Oak Grove Drive, Pasadena, CA, USA

<sup>8</sup> Warsaw University Observatory, Aleje Ujazdowskie 4, 00-478 Warszawa, Poland

cant after accounting for so-called *look-elsewhere* effects,<sup>9</sup> or if they could simply be the product of so-called *a-posteriori* statistical inference<sup>10</sup> (see, e.g., [Bennett et al. 2011](#)). Demonstrating robustness with respect to statistics and data selection can to some extent alleviate such criticisms. With this in mind, we study in this Letter the question of statistical isotropy from the simplest possible point of view, namely by computing the local variance of the CMB fluctuations over patches of different sizes and positions on the sky, and comparing these measurements with those obtained from isotropic simulations. Related variance-oriented studies have been performed for example by [Bernui et al. \(2007\)](#); [Bernui & Hipolito-Ricaldi \(2008\)](#); [Lew \(2008a,b\)](#); [Zhao \(2013\)](#); [Rath & Jain \(2013\)](#); [Gruppuso et al. \(2013\)](#).

## 2. DATA AND METHOD

We include in the following analysis the foreground-reduced co-added V (61 GHz) and W (94 GHz) temperature sky maps from the 9-year *WMAP* data release, and the SMICA map from the *Planck* 2013 data release ([Planck Collaboration 2013b](#)); the three other *Planck* CMB temperature solutions (**Commander-Ruler**, **NILC** and **SEVEM**) give consistent results, and are omitted in the following for brevity. To exclude pixels that are highly contaminated by diffuse foreground emission and point sources, we adopt the *WMAP9* KQ85 Galactic and point source mask, with a sky coverage of  $\sim 75\%$ , for the *WMAP* data, and the *Planck* standardized common mask, U73, with a sky coverage of  $\sim 73\%$  ([Planck Collaboration 2013b](#)), for the *Planck* map.

In order to assess the significance of any anisotropic signal in the data, we resort to simulated isotropic CMB maps. For the *WMAP* case, we generate 1000 CMB-plus-noise Monte Carlo simulations based on the *WMAP9* best-fit  $\Lambda$ CDM power spectrum ([Hinshaw et al. 2013](#)). Noise realizations are drawn as uncorrelated Gaussian realizations with a spatially varying RMS distribution given by the number of observations per pixel; the *WMAP* simulations do not contain lensing effects. For *Planck* we adopt the 1000 “Full Focal Plane” (FFP6) end-to-end simulations produced by the *Planck* collaboration based on the instrument performance and noise properties. The FFP6 CMB and noise maps have been propagated through the *Planck* pipelines with the same weighting as the data. These simulations also incorporate lensing effects and are treated identically to the data in all steps discussed below. The Doppler boosting effects, which have been shown to be an issue on small angular scales (high multipoles; [Planck Collaboration 2013d](#)), have not been taken into account in this anal-

<sup>9</sup> The look-elsewhere effect is a statistical effect that impacts the calculated significance of observing a local excess of events when searching for a signal in a possible range of a particular quantity without knowing a priori where the signal will appear within the range. This is especially severe if the significance is moderate. The significance calculation must account for the fact that an excess anywhere in the range could equally be considered as a signal. Therefore the look-elsewhere effect must be taken care of by taking into account the probability of observing a similar excess anywhere in the range (see, e.g., [Gross & Vitells 2010](#)).

<sup>10</sup> This refers to the cases where an anomalous feature is not predicted by any models before observing the data and is picked arbitrarily only after looking at the data. In other words, the feature is observed because the employed statistical method is designed to detect it.

ysis. However, since variance is more sensitive to large angular scales (low multipoles), our results should not be significantly affected by these effects. We leave a full investigation of the Doppler boosting effects for future work.

The analysis proceeds as follows: We consider 3072 disks (of various sizes) centered on the pixels of a HEALPix  $N_{\text{side}} = 16$  map<sup>11</sup> ([Górski et al. 2005](#)). For each disk and sky map, we compute the temperature variance including only unmasked pixels; any disk for which more than 90% of the area is masked is ignored completely. This results in a low-resolution and almost full-sky map of the local variance across the sky. To establish the expected mean and variance of each disk, we compute the same local-variance map from the simulated ensemble. This mean map is then subtracted from both the observed and simulated local-variance maps, resulting in a zero-mean variance variation map. Finally, we fit a dipole to each of these local-variance maps using the HEALPix `remove_dipole` routine using inverse variance weighting. Note that this procedure is strongly related to the Crossing statistic described by [Shafieloo et al. \(2011\)](#); [Shafieloo \(2012a,b\)](#), which has been applied to isotropy tests with low-redshift supernovae data ([Colin et al. 2011](#)).

## 3. ANALYSIS OF ANISOTROPIC SIMULATIONS

Before we discuss our results for the real data, we assess the sensitivity of the method by applying it to both simulated isotropic and anisotropic CMB realizations. The anisotropic simulations have been modulated by a dipole (Equation (1)) with an amplitude of  $A = 0.072$  and a direction of  $(l, b) = (224^\circ, -22^\circ)$ , consistent with that reported for large angular scales (e.g., [Hoftuft et al. 2009](#)). Two different sets of anisotropic simulations are generated, one for which all scales are modulated, and another for which only scales larger than  $5^\circ$  (corresponding to a  $5^\circ$  smoothing) have been modulated.

Figure 1 shows the resulting local-variance dipole amplitudes (top panel) and directions (bottom panels) as a function of disk radius for each of the 1000 FFP6 simulations, ranging between  $1^\circ$  and  $90^\circ$ .<sup>12</sup> Here we see that the sensitivity of the statistic depends significantly on the disk radius over which the variance is computed, and at a radius of  $\sim 20^\circ$  even the amplitude distribution for the fully modulated model starts to overlap with the isotropic distribution. This makes intuitive sense, since the larger the radius, the more weight is put on the larger angular scales, and hence cosmic variance begins to dominate. For example, a radius of  $20^\circ$  corresponds roughly to angular features of  $\ell \approx 180^\circ/20^\circ \approx 10$ . This correspondence applies independently of the specific details of the assumed anisotropic model, and in the following we therefore restrict our interest to the range between  $1^\circ$  and  $20^\circ$ .

By choosing the disk sizes this way we can also avoid the problems related to a-posteriori statistics and look-elsewhere effects. The choice has been made before ana-

<sup>11</sup> The results are not sensitive to the number of disks, as long as the entire sky is covered, and consistent results are obtained with, say, an  $N_{\text{side}} = 8$  grid.

<sup>12</sup> The directions are shown only for anisotropic simulations; the resulting directions for isotropic simulations are uniformly distributed all over the sky and we do not show them here for brevity.

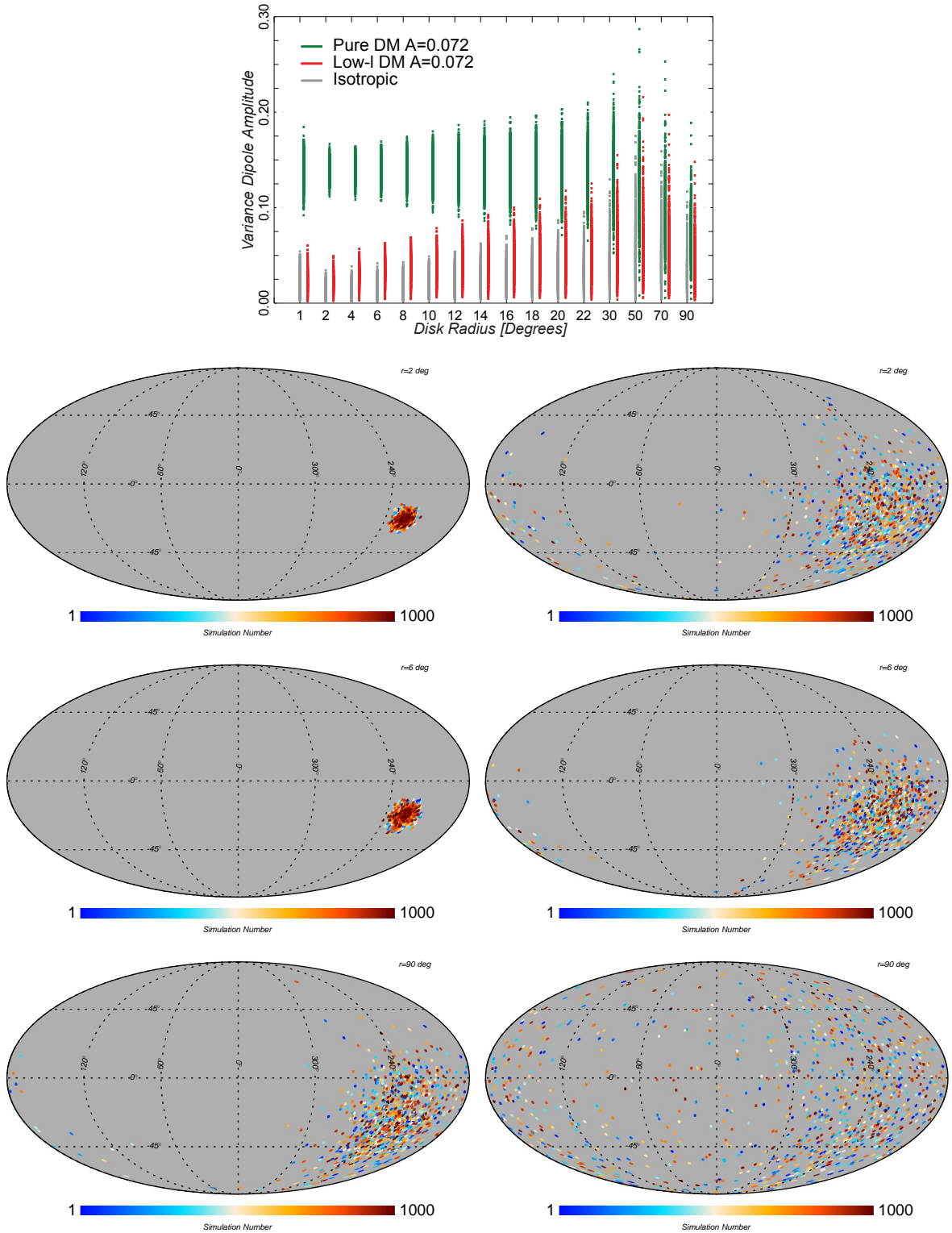


FIG. 1.— Top panel: local-variance dipole amplitude as a function of disk radius for 1000 *Planck* (SMICA) FFP6 isotropic simulations (gray points), as well as for 1000 all-scale dipolar-modulated (pure DM; green points) and low-multipole-only (scales larger than  $5^\circ$ ) dipolar-modulated (low- $l$  DM; red points) simulations. Bottom panel: dipole directions recovered from all-scale (first column) and low-multipole-only (second column) dipolar-modulated simulations with disks of radii  $2^\circ$ ,  $6^\circ$  and  $90^\circ$ . For all cases the input dipole amplitude and directions are  $A = 0.072$  and  $(l, b) = (224^\circ, -22^\circ)$ .

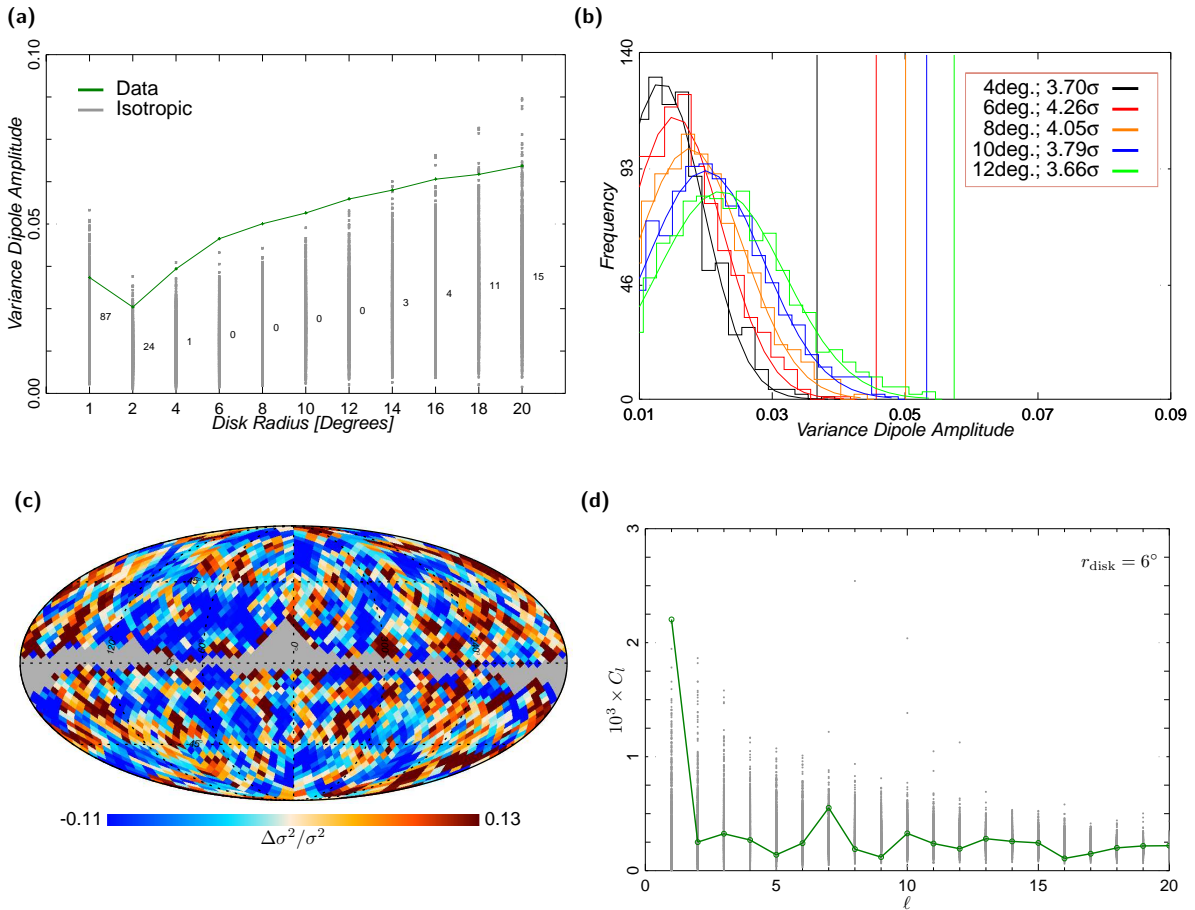


FIG. 2.— (a) Local-variance dipole amplitude as a function of disk radius for *Planck* (SMICA) data (in green) versus the 1000 isotropic FFP6 simulations (in gray). The labels above each scale indicate the number of simulations with amplitudes larger than the ones estimated from the data, and are located at the means of the amplitude values from the simulations. (b) Histograms of the local-variance dipole amplitudes from the 1000 FFP6 simulations for disk radii  $4^\circ$ ,  $6^\circ$ ,  $8^\circ$ ,  $10^\circ$  and  $12^\circ$ , together with the best-fit Gaussian distributions in all cases. Vertical lines indicate the corresponding amplitudes measured from the *Planck* data. The legend shows the rough estimates of detection significances derived from the Gaussian fits. (c) Mean-field subtracted, local-variance map computed with  $6^\circ$  disks for *Planck* (SMICA) data. (d) Angular power spectrum ( $C_\ell$ ) of the local-variance map computed with  $6^\circ$  disks for the 1000 FFP6 simulations (in gray), as well as for *Planck* (SMICA) data (in green).

lyzing the real data, and hence, the results we will present in the next section should not be interpreted as being a-posteriori. In addition, given that we look for the asymmetry signal only using disk sizes that are shown to be sensitive enough, our method is immune from the look-elsewhere criticism. Moreover, since the pixels on the smaller disks belong also to the larger disks, the local-variance dipole amplitudes and directions obtained using disks with different sizes are highly correlated, and this largely reduces the total number of independent statistics used. This therefore further weakens the look-elsewhere effects. One consequence of the disk correlations is that one cannot simply sum the significances from different disk sizes, nor can one use the correlations between different dipole directions to derive a statistical measure as has been done in power-asymmetry analyses Hansen et al. (2009), Axelsson et al. (2013) and Planck Collaboration (2013d).

#### 4. RESULTS

We now apply our variance estimator to the real *WMAP* and *Planck* data. First, Figure 2(a) shows the results for *Planck*, plotted in the same format as in Figure

1, but now comparing with the 1000 FFP6 isotropic simulations. As seen in the plot, none of the 1000 isotropic simulations have local-variance dipole amplitudes larger than the data over the range  $6^\circ \leq r_{\text{disk}} \leq 12^\circ$ , formally corresponding to a lower limit on the statistical significance of  $3.3\sigma$  or a  $p$ -value of 0.001. To give a rough estimate of an actual significance, and not only a lower limit, we plot in Figure 2(b) histograms of the variance dipole amplitudes for the FFP6 simulations at the disk radii with the highest detection significances, and fit a Gaussian in each case. Employing these extrapolations, we derive significances of  $\sim 4\sigma$  in each of these cases. However, we emphasize that these numbers only serve as a rough guide, as the distributions do have significant non-Gaussian tails; an extended ensemble of simulations is certainly preferable over this approximation.

In order to see how a typical local-variance map, for a high-significance detection of asymmetry, looks like, we show in Figure 2(c) the mean-field subtracted map for  $6^\circ$  disks. Figure 2(d) shows the angular power spectrum of the same map as a function of multipoles. This clearly shows that the dipole component is the dominant mode in the local-variance map. Figure 2(d) also indicates that

TABLE 1  
COMPUTED VARIANCE ASYMMETRY SIGNIFICANCES WITH DIFFERENT DISK RADII

Data	Mask	$C_\ell$ Used in Simulations	2°	4°	6°	8°	10°	12°	14°	16°	18°	20°
<i>WMAP9</i>	KQ85	<i>WMAP9</i> best-fit	101	28	7	5	6	6	9	15	20	27
<i>Planck</i> (SMICA)	U73	<i>Planck</i> best-fit	24	1	0	0	0	0	3	4	11	15
<i>WMAP9</i>	KQ85 + U73	<i>WMAP9</i> best-fit	23	3	1	1	3	5	9	13	18	30
<i>Planck</i> (SMICA)	KQ85 + U73	<i>Planck</i> best-fit	16	1	1	0	1	3	7	9	13	22
<i>WMAP9</i>	KQ85	<i>Planck</i> best-fit	98	17	1	0	0	0	0	0	0	0

the data is very consistent with isotropic simulations at all multipoles except for the dipole, which is anomalously large.

Similar results derived from the *WMAP9* observations show qualitatively the same trend, but differ somewhat in terms of final significances (see Table 1). Specifically, a maximum asymmetry is seen between 6° and 12°, with  $\sim 5$  out of 1000 isotropic simulations exhibiting a larger variance dipole amplitude, for a  $p$ -value of  $\sim 0.005$  and a statistical significance of  $\sim 2.9\sigma$ .

The preferred directions obtained in the present Letter (for 8° disks) are listed in Table 2, together with a number of similar results obtained in previous papers, and summarized visually in Figure 3.<sup>13</sup> Clearly, the preferred directions derived by very different algorithms and data combinations are all in good qualitative agreement.

*Ecliptic variance asymmetry.*— Before we end this section, we present the results of a different, but related study, using variance as the statistic, which we have performed in addition to the main analysis of this Letter. In Planck Collaboration (2013d) it is reported that the variances of the CMB fluctuations computed on the northern ecliptic and Galactic hemispheres are significantly smaller compared to the corresponding southern ones. We repeated the same analysis here, for the ecliptic hemispheres, and obtained similar results. A potential criticism of this study is the fact that it ignores look-elsewhere effects. This can be dealt with by using a test statistic, based on the differences in variances between different hemispheres, that involves a ranking procedure. Specifically, we first compute the difference in variances for each pair of opposite hemispheres for the data. By sorting the obtained values we assign a rank to for example the northern-southern ecliptic hemispheres. We then compare this value to the values with the same rank obtained from repeating the same procedure to all isotropic simulations, and derive a  $p$ -value. The  $p$ -value we obtain this way for the *Planck* data and FFP6 simulations shows that the variance difference along the ecliptic pole for the data is not significantly different from that of the isotropic simulations. However, performing the same procedure on the variance values for hemispheres (and not the variance differences) indicates that the variance

<sup>13</sup> Note that no dipole modulation results have been published for the 9-year *WMAP* temperature sky maps to date. However, given that the 9-year *WMAP* sky maps are virtually indistinguishable from the 5-year sky maps on angular scales larger than 5° relative to cosmic variance, we expect the dipole modulation results to be very close to those reported by Hoftuft et al. (2009) for the 5-year *WMAP* data.

TABLE 2  
ASYMMETRY DIRECTIONS

Map	$(l,b)$ [°]	Significance or $p$ -value	Reference
<i>Planck</i> -VA <sup>a</sup>	(212, -13)	0/1000	Present work
<i>WMAP9</i> -VA	(219, -24)	5/1000	Present work
<i>Planck</i> -DM	(227, -15)	3.5 $\sigma$	Planck Collaboration (2013d)
<i>WMAP5</i> -DM	(224, -22)	3.3 $\sigma$	Hoftuft et al. (2009)
<i>Planck</i> -PA	(218, -21)	0/500	Planck Collaboration (2013d)
<i>WMAP9</i> -PA	(227, -27)	7/10000	Axelsson et al. (2013)

<sup>a</sup>VA, DM and PA stand for variance asymmetry, dipole modulation and power asymmetry, respectively.

from the northern ecliptic hemisphere for the data is still significantly low with a  $p$ -value of 4/1000. Using ratios of variances instead of differences in variances has no impact on our results.

## 5. SUMMARY

We have applied a simple local-variance estimator to the latest *WMAP* and *Planck* data, performing a frequentist test of global statistical isotropy. For the *Planck* data, we find that the local variance exhibits dipolar-like spatial variations that are statistically significant (at least) at the  $\sim 3\sigma - 3.5\sigma$  level on scales between  $\sim 4^\circ$  and  $14^\circ$  by this measurement. For *WMAP*, we find a statistical significance of  $\sim 2.9\sigma$ , and a direction fully consistent with that derived from *Planck*.

The results obtained here are in good qualitative agreement with earlier results, for example using direct likelihood fits or bipolar harmonics (Hoftuft et al. 2009; Planck Collaboration 2013d), that indicate a  $\gtrsim 3\sigma$  dipole-modulation-like effect on large angular scales, but with an amplitude that is decreasing with angular scale. In the present approach, this is seen by the fact that the statistical significance decreases for the smallest disk radii of  $1^\circ - 2^\circ$  scales; for a pure dipole modulation extending through all multipoles this stays constant.

The slight difference between *Planck* and *WMAP* can be mainly explained by the different masks that have been used in the two cases. In order to study the effects of the masks on the results, we repeated the analysis for both the *WMAP* and *Planck* maps using a unified mask, i.e. the combination of the *Planck* U73 and *WMAP9* KQ85 masks. We obtained very similar results in these cases (see Table 1). The remaining differences can be at least partially explained by the different noise levels

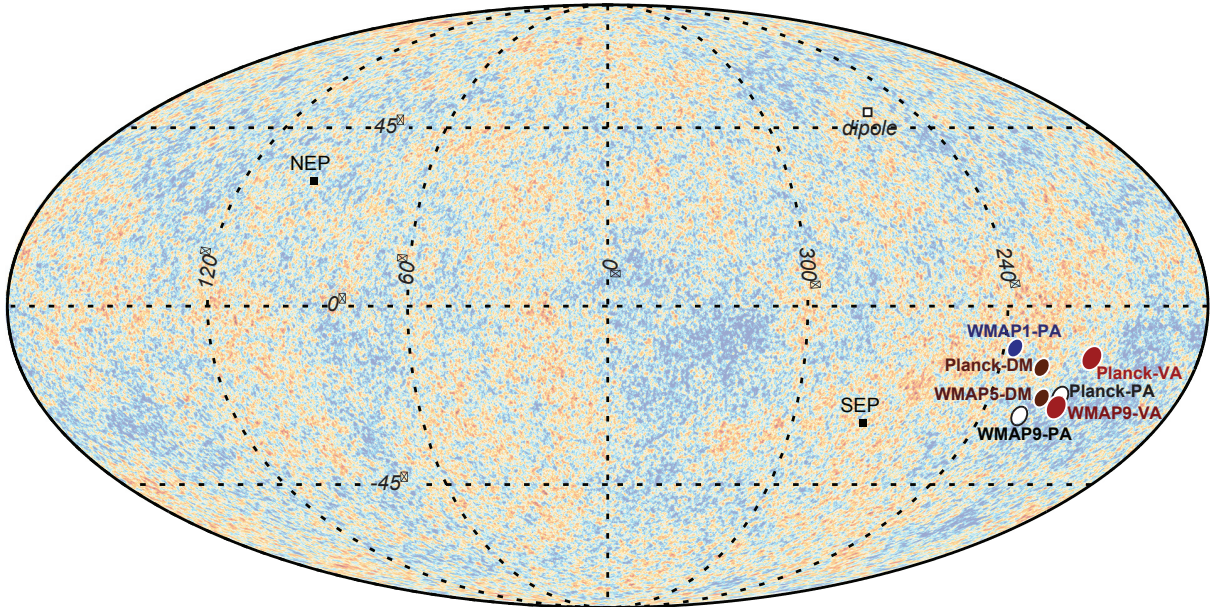


FIG. 3.— Asymmetry directions found in this work by analyzing the local variance of the *WMAP* 9-year and *Planck* 2013 data [denoted by *WMAP9-VA* and *Planck-VA*], as well as the directions found previously from the latest likelihood analyses of the dipole modulation model [denoted by *WMAP5-DM* (Hoftuft et al. 2009) and *Planck-DM* (Planck Collaboration 2013d)] and the local-power spectrum analyses [denoted by *WMAP1-PA* (Eriksen et al. 2004), *WMAP9-PA* (Axelsson et al. 2013) and *Planck-PA* (Planck Collaboration 2013d)] for the *WMAP* and *Planck* data. The background map is the CMB sky observed by *Planck* (SMICA). VA, DM and PA stand for variance asymmetry, dipole modulation and power asymmetry, respectively.

of the two experiments. No smoothing is applied to either data set in this analysis, and the variance therefore receives a significant contribution from the pixel-scale noise, which is substantially larger for *WMAP* than for *Planck*, decreasing the effective sensitivity of the estimator.

One should note however that choosing the right theoretical angular power spectrum for the isotropic simulations of the CMB maps is crucial and can also impact the obtained statistical significances, and might therefore provide another explanation for the differences in the significances computed from *WMAP* and *Planck*. It is known that (Planck Collaboration 2013c) there is a 1% – 2% mismatch between the power spectra computed from the two data sets and this can potentially explain some of the discrepancy that we see here. We have tested this effect by using the *Planck* best-fit power spectrum (Planck Collaboration 2013c) to generate the simulations for *WMAP*. We observe that enforcing the *Planck* spectrum on the *WMAP* data makes the *WMAP* results comparable with the *Planck* ones. The significances for *WMAP* are now 0/1000 over disk radii of  $8^\circ - 22^\circ$  (see Table 1), while the dipole directions do not change. This suggests, and remains to be investigated, that after resolving the tension between the *Planck* and *WMAP* power spectra the results of our analysis for the two experiments will agree better.

In this Letter we have focused on dipolar variations in

the local-variance map, but this is clearly easily generalizable to higher-order modes. This will be considered in future work. For now, we note that the main advantages of the method are its conceptual and implementational simplicity, its directly intuitive interpretation, and, by virtue of being defined in pixel space, a useful complementarity to other typically harmonic-based methods. The fact that different statistical techniques, with different properties and sensitivities, result in very similar conclusions does weaken the suggestion that the effect is simply the product of a-posteriori statistics.

We thank Claudio Llinares, Eamon M. Scullion and Amir Hajian for helpful discussions. Y.A. and H.K.E. acknowledge support through the ERC Starting Grant StG2010-257080. Y.F. is supported by ERC Grant 277742 Pascal. A.S. thanks the Korean Ministry of Education, Science and Technology (MEST), Gyeongsangbuk-Do and Pohang City for the support of the Independent Junior Research Groups at the Asia Pacific Center for Theoretical Physics (APCTP). F.K.H. acknowledges OYI grant from the Norwegian research council. We acknowledge the use of resources from the Norwegian national super-computing facilities, NOTUR. Maps and results have been derived using the HEALPix (<http://healpix.jpl.nasa.gov>) software package developed by Górski et al. (2005).

#### REFERENCES

- Abolhasani, A. A., Baghran, S., Firouzjahi, H., & Namjoo, M. H. 2014, *Phys.Rev.*, D89, 063511  
 Axelsson, M., Fantaye, Y., Hansen, F., et al. 2013, *Astrophys.J.*, 773, L3  
 Bennett, C. L., Halpern, M., Hinshaw, G., et al. 2003, *ApJS*, 148, 1  
 Bennett, C. L., Hill, R. S., Hinshaw, G., et al. 2011, *ApJS*, 192, 17  
 Bernui, A., & Hipolito-Ricaldi, W. 2008, *Mon.Not.Roy.Astron.Soc.*, 389, 1453  
 Bernui, A., Mota, B., Rebouças, M. J., & Tavakol, R. 2007, *Astron.Astrophys.*, 464, 479

- Bridges, M., McEwen, J., Lasenby, A., & Hobson, M. 2007, *Mon.Not.Roy.Astron.Soc.*, 377, 1473
- Cai, Y.-F., Zhao, W., & Zhang, Y. 2014, *Phys.Rev.*, D89, 023005
- Colin, J., Mohayaee, R., Sarkar, S., & Shafieloo, A. 2011, *Mon.Not.Roy.Astron.Soc.*, 414, 264
- Copi, C., Huterer, D., Schwarz, D., & Starkman, G. 2007, *Phys.Rev.*, D75, 023507
- Cruz, M., Cayon, L., Martinez-Gonzalez, E., Vielva, P., & Jin, J. 2007, *Astrophys.J.*, 655, 11
- Dai, L., Jeong, D., Kamionkowski, M., & Chluba, J. 2013, *Phys.Rev.*, D87, 123005
- de Oliveira-Costa, A., Tegmark, M., Zaldarriaga, M., & Hamilton, A. 2004, *Phys.Rev.*, D69, 063516
- Erickeek, A. L., Kamionkowski, M., & Carroll, S. M. 2008, *Phys.Rev.*, D78, 123520
- Eriksen, H. K., Banday, A., Gorski, K., Hansen, F., & Lilje, P. 2007, *Astrophys.J.*, 660, L81
- Eriksen, H. K., Hansen, F. K., Banday, A. J., Gorski, K. M., & Lilje, P. B. 2004, *ApJ*, 605, 14
- Planck Collaboration 2013a, arXiv:1303.5062
- . 2013b, arXiv:1303.5072
- . 2013c, arXiv:1303.5075
- . 2013d, arXiv:1303.5083
- Gordon, C., Hu, W., Huterer, D., & Crawford, T. 2005, *Phys. Rev. D*, 72, 103002
- Górski, K. M., Hivon, E., Banday, A. J., et al. 2005, *ApJ*, 699, 759
- Gross, E., & Vitells, O. 2010, *European Physical Journal C*, 70, 525
- Gruppuso, A. 2013, *JCAP*, 1307, 047
- Hajian, A., & Souradeep, T. 2003, *Astrophys.J.*, 597, L5
- . 2006, *Phys.Rev.*, D74, 123521
- Hansen, F. K., Banday, A. J., & Górski, K. M. 2004, *MNRAS*, 354, 641
- Hansen, F. K., Banday, A. J., Gorski, K. M., Eriksen, H. K., & Lilje, P. B. 2009, *ApJ*, 704, 1448
- Hinshaw, G., et al. 2007, *Astrophys.J.Suppl.*, 170, 288
- . 2013, *Astrophys.J.Suppl.*, 208, 19
- Hoftuft, J., Eriksen, H. K., Banday, A. J., et al. 2009, *ApJ*, 699, 985
- Jaffe, T., Banday, A., Eriksen, H., Gorski, K., & Hansen, F. 2006, *Astron.Astrophys.*, 460, 393
- Kanno, S., Sasaki, M., & Tanaka, T. 2013, *PTEP*, 111E01
- Kohri, K., Lin, C.-M., & Matsuda, T. 2013, arXiv:1308.5790
- Land, K., & Magueijo, J. 2005a, *Mon.Not.Roy.Astron.Soc.*, 357, 994
- . 2005b, *Phys.Rev.Lett.*, 95, 071301
- . 2007, *Mon.Not.Roy.Astron.Soc.*, 378, 153
- Larson, D. L., & Wandelt, B. D. 2004, *Astrophys.J.*, 613, L85
- Lew, B. 2008a, *JCAP*, 0809, 023
- . 2008b, *JCAP*, 0808, 017
- Liddle, A. R., & Corts, M. 2013, *Phys.Rev.Lett.* 111, 111302
- Liu, Z. G., Guo, Z. K., & Piao, Y. S. 2013, *Phys.Rev.*, D88, 063539
- Lyth, D. H. 2013, *JCAP*, 1308, 007
- Mazumdar, A., & Wang, L. 2013, *JCAP*, 1310, 049
- McDonald, J. 2013, *JCAP*, 1311, 041
- McEwen, J. D., Hobson, M., Lasenby, A., & Mortlock, D. 2005, *Mon.Not.Roy.Astron.Soc.*, 359, 1583
- . 2006, *Mon.Not.Roy.Astron.Soc.*, 371, L50
- Namjoo, M. H., Baghran, S., & Firouzjahi, H. 2013, *Phys.Rev.*, D88, 083527
- Park, C. G. 2004, *MNRAS*, 349, 313
- Pietrobon, D., Amblard, A., Balbi, A., et al. 2008, *Phys.Rev.*, D78, 103504
- Rath, P. K., & Jain, P. 2013, *JCAP*, 1312, 014
- Shafieloo, A. 2012a, *JCAP*, 1205, 024
- . 2012b, *JCAP*, 1208, 002
- Shafieloo, A., Clifton, T., & Ferreira, P. G. 2011, *JCAP*, 1108, 017
- Spergel, D., et al. 2007, *Astrophys.J.Suppl.*, 170, 377
- Tegmark, M., de Oliveira-Costa, A., & Hamilton, A. 2003, *Phys.Rev.*, D68, 123523
- Vielva, P., Martinez-Gonzalez, E., Barreiro, R., Sanz, J., & Cayon, L. 2004, *Astrophys.J.*, 609, 22
- Zhao, W. 2013, *Mon.Not.Roy.Astron.Soc.*, 433, 3498-3505